

FIRST RESULTS FROM THE FAINT OBJECT CAMERA:¹ OBSERVATIONS OF PKS 0521–36

F. MACCHETTO,^{2,3,4} R. ALBRECHT,^{2,3,5,6} C. BARBIERI,^{2,7} J. C. BLADES,^{2,4} A. BOKSEBERG,^{2,8} P. CRANE,^{1,6}
 J. M. DEHARVENG,^{2,9} M. J. DISNEY,^{2,10} P. JAKOBSEN^{2,11} T. M. KAMPERMAN^{2,12} I. R. KING,^{2,13}
 C. D. MACKAY,^{2,14} F. PARESCHE,^{2,3,4} G. WEIGELT,^{2,15} D. BAXTER,⁴ P. GREENFIELD,⁴
 R. JEDRZEJEWSKI,⁴ A. NOTA,^{4,7} AND W. B. SPARKS⁴

Received 1990 October 15; accepted 1990 November 16

ABSTRACT

The Faint Object Camera on the *Hubble Space Telescope* was used to observe the radio galaxy PKS 0521–36 which hosts a prominent radio jet. Images of the jet show spatial structure comparable to VLA data and significantly better than optical ground-based observations. The jet structure is resolved at FOC resolution. In addition to the radio knot, well resolved by the FOC, an extension of the jet toward the nucleus is apparent. The rest of the jet does not show much clumpiness, implying that the synchrotron electrons must be accelerated all along the jet to account for the extent in the optical region.

Subject headings: galaxies: individual (PKS 0521–36) — galaxies: jets — radio sources: galaxies

1. INTRODUCTION

The Faint Object Camera (FOC) is part of the European Space Agency's contribution to the NASA and ESA collaboration on the *Hubble Space Telescope* (*HST*). The FOC was designed to take full advantage of the increased spatial resolution provided by the *HST* optics (Macchetto et al. 1980; Macchetto 1982; Paresce 1990) particularly in the ultraviolet and optical spectral region. The FOC has two independent optical relays, at $f/96$ and $f/48$, which magnify and refocus the incoming light onto separate but identical two-dimensional photon counting detectors. Each detector works typically with 512×512 pixels (although other modes can be used), and each $25 \mu\text{m}$ pixel covers 0.022 arcsec^2 or 0.044 arcsec^2 in the sky.

To determine the effect of the telescope's spherical aberration on the capabilities of *HST*'s scientific instruments, a short program of observations, derived from the approved scientific programs of each Investigation Definition Team, was estab-

lished and carried out. The results reported in this and the other FOC papers in this issue arise from this science assessment program.

The study of the optical counterparts of radio jets will be the subject of an intensive investigation program with the FOC first proposed 10 years ago (Miley 1981; Macchetto 1981). Radio jets are observed in hundreds of radio galaxies and quasars (e.g., van Breugel & Miley 1977; Miley 1980), and they are known to play a fundamental role in the transport of energy from the nucleus to the radio-emitting lobes (Rees 1971). Despite extensive searches, only a very small number of radio jets have been detected in the optical region (e.g., Butcher, van Breugel, & Miley 1980; Keel 1988). One of the most prominent radio and optical jets is that found in the elliptical galaxy PKS 0521–36, a relatively isolated elliptical radio galaxy at a redshift $z = 0.055$ which also harbors a bright $V = 16$ BL Lac nucleus and extended optical line emission. Detailed spectroscopic and morphological studies have been carried out by Danziger et al. (1979, 1983); Cayatte & Sol (1987); and Boisson, Cayatte, & Sol (1989). Recently Sparks, Miley, & Macchetto (1990) reported optical polarization measurements of the jet and nucleus, which confirmed the expected high polarization if the emission is due to synchrotron radiation.

High spatial resolution optical observations offer the possibility, due to the extremely short electron lifetime, of precisely determining locations within the jet where particle acceleration occurs, and by comparing to radio maps of similar resolution of investigating viable confinement mechanisms and diffusion processes within the relativistic plasma. The extensive data and our expectation of being able to carry out direct comparison of the VLA data (Keel 1986), together with the challenge of the bright nucleus and intrinsic scientific interest of the target, made PKS 0521–36 a good candidate for the FOC science assessment observations.

2. OBSERVATIONS AND REDUCTIONS

Images of PKS 0521–36 were obtained on 1990 August 25 using the F430W and F320W filters and $f/96$, 512×512 mode (Paresce 1990) with a corresponding pixel size approximately $0''.022$. Pointing was defined using the radio VLBI positions obtained by Morabito et al. (1986). Exposures were made in

¹ Based on observations with the NASA/ESA *Hubble Space Telescope*, obtained at the Space Telescope Science Institute, which is operated by AURA, Inc., under NASA contract NAS 5-26555.

² Member FOC Investigation Definition Team.

³ Astrophysics Division, Space Science Department of ESA.

⁴ Space Telescope Science Institute, 3700 San Martin Drive, Baltimore, MD 21218.

⁵ Space Telescope European Coordinating Facility.

⁶ European Southern Observatory, Karl Schwarzschild Strasse 2, D-8096 Garching, Federal Republic of Germany.

⁷ Osservatorio Astronomico di Padova, Vicolo Osservatorio, 5, I-35122 Padova, Italy.

⁸ Royal Greenwich Observatory, Madingley Road, Cambridge CB3 0EZ, United Kingdom.

⁹ Laboratoire d'Astronomie Spatiale du CNRS, Traverse du Siphon, Les Trois Lucs, F-13012, Marseille, France.

¹⁰ Department of Physics, University College of Cardiff, PO Box 713, Cardiff CF1 3TH, Wales, United Kingdom.

¹¹ Astrophysics Division, Space Science Department of ESA, ESTEC, NL-2210 AG, Noordwijk, The Netherlands.

¹² Laboratory for Space Research, Utrecht, Space Research Institute, Beneluxlaan 21, NL-3527 MS Utrecht, The Netherlands.

¹³ Astronomy Department, University of California, Berkeley, Berkeley, CA 94720.

¹⁴ Institute of Astronomy, Cambridge, Madingley Road, Cambridge CB3 0HA, United Kingdom.

¹⁵ Max-Planck-Institut für Radioastronomie, Auf dem Hügel 69, D-5300 Bonn 1, Federal Republic of Germany.

fine lock, with an expected tracking accuracy of $0''.007$ during the exposures. The exposures were of nominal duration of 1500 s, two in each filter. Approximately 10% of the integration time was lost due to loss of fine-lock, caused by spacecraft jitter during day/night terminator crossings.

The data were processed by correcting for electron–optically induced distortion using a grid of regularly spaced reseau marks on the faceplate of the detector, giving a final pixel scale of $\approx 0''.022$ pixel $^{-1}$. Internal flat-field LED exposures were processed in the same way, and the data frames were divided by normalized geometrically corrected flat-field frames. This procedure is flux-conserving.

The galaxy has a very bright, $V \approx 16$, BL Lac nucleus which severely tests the ability of *HST* and the FOC to detect faint structure in the vicinity of bright objects. Accurate knowledge of the point-spread function appropriate to the data is essential to remove the halo around the nucleus which arises from the presence of spherical aberration in the *HST* primary mirror.

Various techniques were tried to remove the effects of the nucleus, from straightforward subtraction of a scaled point-spread function (PSF), direct Fourier deconvolution, maximum entropy deconvolution, and Lucy's (1974) iterative deconvolution technique. A combination of point source subtraction and Lucy's method gave the best results. Specific PSF observations were obtained of the star BPM 16274, a UV flux standard (Bohlin et al. 1990; Turnshek et al. 1990); however, these data were only obtained some weeks after the original observations of PKS 0521–36. Potential mismatches between the data and stellar PSF also arise because of the large color difference between these objects. A second PSF was therefore derived from observations of the BL Lac object AP Lib that had been observed the day preceding the observations of PKS 0521–36 and which provides a much better color match. This was constructed from two images which combined the unsaturated core of one with the higher signal-to-noise ratio wings of the other. Although there is clearly some contamination of that PSF due to the host galaxy of AP Lib, it is small compared with the point source itself. Only the F430W filter was used in common to both of these sets of data.

An example of the resultant deconvolutions is shown in Figure 1 (Plate L16). This uses Lucy's (1974) iterative deconvolution technique which constrains the result to be positive. To obtain better convergence and discrimination of the nucleus, a point source of luminosity equal to 75% of the nuclear luminosity was first subtracted. Convergence, defined by a reduced chi-squared value between the data and model of less than or equal to 1, was achieved fairly quickly, in about 10 iterations. The resultant resolution is a function of the signal-to-noise ratio—in the nucleus we resolve structure on scales $0''.1$, while in the jet $0''.2$ – $0''.3$ is a realistic estimate of the resolution. A model of the underlying galaxy has also been subtracted in Figure 1, in order to show the jet more clearly. The BL Lac nucleus is extremely bright compared with the rest of the image, and the residual structure within $\approx 2''$ is contaminated by the imperfectly removed halo around the point source.

3. RESULTS

The VLA contour data as published by Keel (1986) is shown superposed on the FOC data in Figure 2 (Plate L17). It is immediately obvious that the FOC data has a resolution very similar to that of the VLA data but shows considerably more morphological information than the ground-based optical

data (see, e.g., Sparks et al. 1990 for a high spatial resolution ground-based image).

The FOC image shows a bright knot located $\approx 1''.8$ to the NE and clearly resolved as in the VLA data. The width of the knot is $\approx 0''.8$. Beyond this bright knot, the jet has approximately constant surface brightness and a morphology similar to the VLA image with a total length of $6''.5$. The jet is also resolved in width, $0''.6$ wide in the fainter regions of the jet, with little or no evidence of structure on a scale of $\leq 0''.1$. The FOC data appears to show more flux than the VLA data in the region at slightly larger radius from the nucleus but close to the southern tip of the knot. The signal-to-noise ratio is very low, however, and this requires confirmation. Note that the data in Keel's (1986) Figure 6 does show some low-level emission in this region.

There is a second component seen in the deconvolution at $0''.36$ from the nucleus, Figure 2. It is visible in the raw data, although by no means as clearly as in the deconvolved image. Such a source would be completely within the core of the highest resolution VLA contour map published by Keel. A potential concern is that this second component is an artifact of deconvolution close to the saturated nucleus. We do not expect saturation effects to propagate as far as $0''.36$, but to test this possibility, a saturated image of AP Lib was reduced in similar fashion. No corresponding secondary component was seen. Our tentative conclusion therefore is that we have detected a previously unseen inner jet structure at a distance corresponding to 300 pc, $H_0 = 75$ km s $^{-1}$ Mpc $^{-1}$.

In the acquisition image, namely the image used to define the pointing of the *HST*, we can just detect the "red tip," namely a distinct knot off the jet tip at a distance of some $2''$. It appears as a diffuse faint object. Since it does not have a VLA counterpart, it is unclear whether it is associated with the jet or is a chance spatial coincidence with a foreground or background object. Near-infrared measurements are needed to clarify this point.

4. DISCUSSION

FOC observations of the nucleus of PKS 0521–36 seem to have resolved it into a bright nucleus and an inner jet extension. Presumably the optical polarization measured by Sparks et al. (1990) comes from both these components. The fact that the nuclear polarization is large and perpendicular to the jet direction (Sparks et al. 1990; Angel & Stockman 1980; Bailey, Hough, & Axon 1983; Bridle et al. 1986) is consistent with what has been observed in other quiescent blazars and quasars. The second component close to the nucleus may be an inner extension of the jet since it lies on the geometrical projection of the jet toward the nucleus. However, since this extension falls entirely within the VLA radio core, there is no independent way of confirming its existence. If real, it could be a site of electron acceleration along the jet due to transverse shocks (Drury 1983; Blandford & Eichler 1987).

The large bright knot further along the jet is a clear counterpart to the radio knot. The radio and optical polarization position angles (Keel 1986; Sparks et al. 1990) suggest a magnetic field aligned along the jet direction. This knot is unresolved in the optical polarimetric measurements, but the general sense of the magnetic field is still along the jet direction at that position. The bright knot is clearly an important site where particle acceleration is occurring.

The general optical morphology of the jet does not exhibit any significant degree of clumpiness even at FOC resolution.

PLATE L16

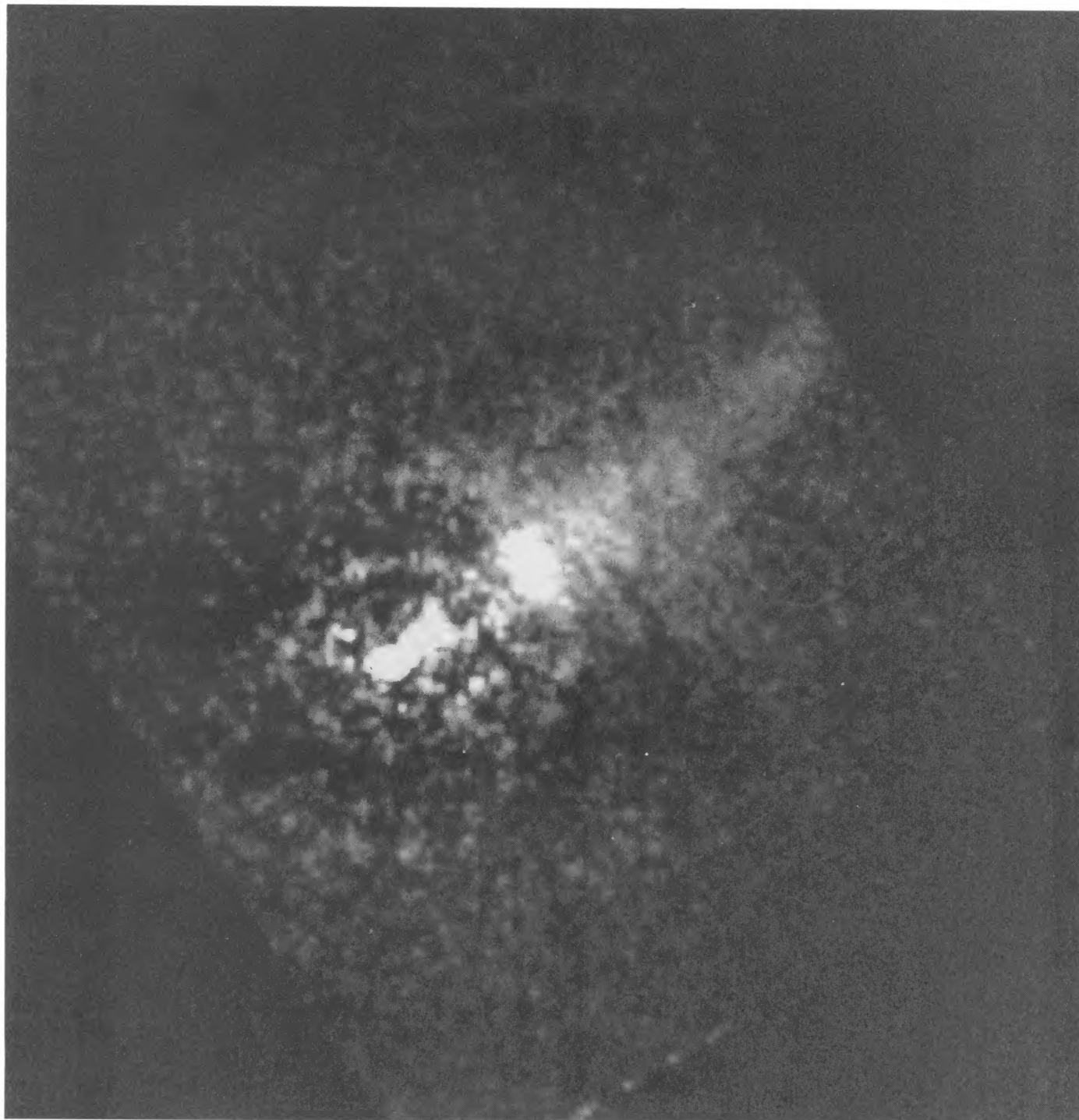


FIG. 1.—The jet in PKS 0521 – 36 as observed by the Faint Object Camera. An elliptical model of the galaxy has been subtracted. The jet is approximately $6''.5$ long.

MACCHETTO et al. (see 369, L56)

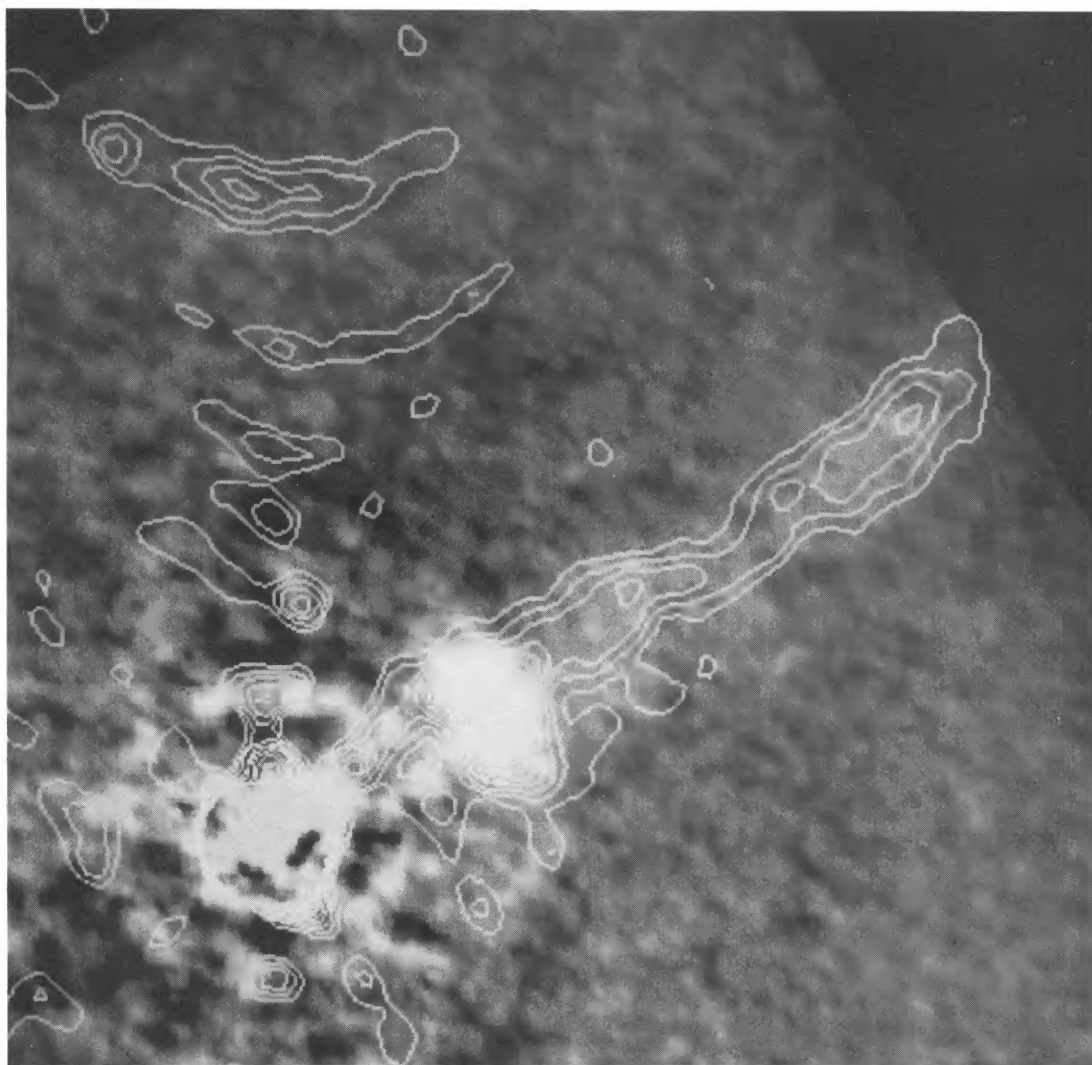


FIG. 2.—The VLA contour data of Keel (1986) is shown superposed on the FOC data. Note the excellent agreement of the two data sets.

MACCHETTO et al. (see 369, L56)

Using the standard formula of Rybicki & Lightman (1979), we derive a mean lifetime for the electrons:

$$t_{1/2} = 16.4 \frac{1}{B^2 \gamma} \text{ yr},$$

where B is the magnetic field in Gauss and γ is the Lorentz factor. The mean distance for electron diffusion is

$$D_{1/2} \approx \frac{5.5}{B^{3/2} v^{1/2}} \text{ kpc}$$

where $v = 120B\gamma^2/10^{-4}$ is the cut-off frequency. With typical value $B \approx 10^{-4}$, the electron diffusion distance is $D \approx 200$ pc in the optical and $D \approx 100$ kpc in the radio region. The corresponding lifetime for the optical electrons is $t_{1/2} \approx 600$ yr. This implies that there must be continuous acceleration along the jet of the electrons responsible for the optical emission, since electron diffusion from the bright knot could not account for the observed optical extent. These results are comparable to values derived for the optical jet in M87 (Fraix-Burnet et al. 1989).

We clearly need higher signal-to-noise ratio observations of this and other optical jets to answer some of the key questions

associated with the optical counterparts to radio jets. What is the role of beaming and orientation in determining the appearance of an optical jet? Is a higher level of nuclear activity at present correlated with the optical jet appearance? What are the electron acceleration and transport mechanisms in these jets? *HST* in fact offers the possibility of having images with higher spatial resolution than the VLA and allowing therefore an excellent probe of physical conditions at particle acceleration sites and of electron diffusion length scales.

The Faint Object Camera is the result of many years of hard work and important contributions by a number of highly dedicated individuals. In particular, we wish to thank ESA *HST* Project Manager Robin Laurance, the ESA/*HST* Project Team and the European contractors for building an outstanding scientific instrument. The FOC IDT Support Team, D. Baxter, P. Greenfield, R. Jedrzejewski, and W. B. Sparks, acknowledge support from ESA through contract 6500/85/NL/SK. P. Crane and I. R. King acknowledge support from NASA through contracts NAS5-27760 and NAS5-28086. The radio VLA data used in Figure 2 were kindly made available to us by Bill Keel.

REFERENCES

- Angel, J. R. P., & Stockman, H. S. 1980, *ARA&A*, 18, 321
 Bailey, J., Hough, J. H., & Axon, D. J. 1983, *MNRAS*, 203, 339
 Blandford, R. D., & Eichler, D. 1987, *Phys. Rept.*, 154, 1
 Bohlin, R. C., Harris, A. W., Holm, A. V., & Gary, C. 1990, *ApJS*, 73, 413
 Boisson, C., Cayatte, V., & Sol, H. 1989, *A&A*, 211, 275
 Bridle, C., Hough, J. H., Bailey, J., Axon, D. J., & Hyland, A. R. 1986, *MNRAS*, 221, 739
 Butcher, H. R., van Breugel, W. J. M., & Miley, G. K. 1980, *ApJ*, 235, 749
 Cayatte, V., & Sol, H. 1987, *A&A*, 171, 25
 Danziger, I. J., Ekers, R. D., Goss, W. M., & Shaver, P. A. 1983, in *Astrophysical Jets*, ed. A. Ferrari & A. G. Pacholczyk (Dordrecht: Reidel), 131
 Danziger, I. J., Fosbury, R. A. E., Goss, W. M., & Ekers, R. D. 1979, *MNRAS*, 188, 415
 Drury, L. O. C. 1983, *Rep. Progr. Phys.*, 46, 973
 Fraix-Burnet, D., Nieto, J.-L., Lelievre, G., Macchetto, F., Perryman, M. A. C., & di Serego Alighieri, S. 1989, *ApJ*, 336, 121
 Keel, W. C. 1986, *ApJ*, 302, 296
 ———. 1988, *ApJ*, 329, 532
 Lucy, L. B. 1974, *AJ*, 79, 745
 Macchetto, F. 1981, in *Proc. of ESO/ESA Workshop Optical Jets in Galaxies*, ed. F. Macchetto, G. Miley, & M. Tarenghi (Noordwijk: ESA), 15
 ———. 1982, in *The Space Telescope Observatory (IAU 18th General Assembly)*, ed. D. N. B. Hall (Greenbelt: NASA), 40
 Macchetto, F., van de Hulst, H. C., di Serego Alighieri, S., & Perryman, M. A. C. 1980, *The Faint Object Camera for the Space Telescope (ESA SP-1028)*
 Miley, G. K. 1980, *A&A*, 18, 165
 ———. 1981, in *Proc. of ESO/ESA Workshop Optical Jets in Galaxies*, ed. F. Macchetto, G. Miley, & M. Tarenghi (Noordwijk: ESA), 9
 Morabito, D. D., Preston, R. A., Linfield, R. P., Slade, M. A., & Jauncey, D. L. 1986, *AJ*, 92, 546
 Paresce, F. 1990, *FOC Instrument Handbook*, Space Telescope Science Institute
 Rees, M. J. 1971, *Nature*, 229, 312
 Rybicki, G. B., & Lightman, A. P. 1979, *Radiative Processes in Astrophysics* (New York: Wiley)
 Sparks, W., Miley, G., & Macchetto, F. 1990, *ApJ*, 361, L41
 Turnshek, D. A., Bohlin, R. C., Williamson, R. L., Lupie, O. L., Koornneef, J., & Morgan, D. H. 1990, *AJ*, 99, 1243
 van Breugel, W. J. M., & Miley, G. K. 1977, *Nature*, 266, 315
 Wierick, G. 1981, in *Optical Jets in Galaxies (ESA SP-162)*, 29